Well Configurations in Anisotropic Reservoirs

M.J. Economides, SPE, Texas A&M U., and **C.W. Brand** and **T.P. Frick,*** SPE, Mining U. Leoben

Summary

Horizontal wells have emerged as a new means for well-productivity enhancement. Simultaneously, they have brought forward the need to recognize and account for permeability anisotropies, including vertical-to-horizontal and horizontal-to-horizontal directions. In addition, there is the possibility of multiple horizontal drainholes emanating from the same vertical well. Performance relationships for the most interesting well configurations are presented, including both early-time and late-time differences rather than only bounded flow regimes. Solutions for arbitrarily oriented single or multiple horizontal wells are introduced, along with a discussion of well-known existing relationships.

Introduction

It is a foregone conclusion that horizontal wells will capture an ever increasing share of all petroleum wells drilled. The performance of these wells depends greatly on appropriate reservoir selection, substantial predrilling formation evaluation, and optimized completion and stimulation practices.

There have been several attempts to describe and estimate horizontal well-productivity and/or injectivity indexes, and several models have been used for this purpose. Following the tradition of vertical well-productivity models, analogous well and reservoir geometries have been considered. A widely used approximation for the well drainage is, conveniently, a parallelepiped model with no-flow or constant-pressure boundaries at the top or bottom, and either no-flow or infinite-acting boundaries at the sides.

One of the earliest models was introduced first by Borisov,[1] which assumed a constant pressure drainage ellipse whose dimensions depend on the well length. This configuration evolved into a widely used equation presented by Joshi,[2] which accounted for vertical-to-horizontal permeability anisotropy and, adjusted by Economides *et al.*,[3] for a wellbore in elliptical coordinates.

This model, while useful for first approximations and comparisons with vertical well-productivity indexes, does not account for either early-time or late-time phenomena nor, more importantly, realistic well and reservoir configurations.

Babu and Odeh[4] used an expression for the pressure drop at any point by integrating appropriate point source (Green's) functions in space and time. Their solutions for various no-flow boundary positions include infinite-sum expressions, accounting for individual pseudosteady-state pressure drops. These forms are rather complicated and cumbersome to calculate.

Using vertical well analogs, Babu and Odeh[4] grouped their solutions into reservoir/well configuration shape factors and a (horizontal) partial penetration skin effect. This work is in line with the classic Dietz[5] factors that were incorporated for vertical well performance in the Matthews, Bronz and Hazebroek's[6] work. In all cases, the Babu and Odeh[4] work assumes that the well is parallel to the *y*-axis of the parallelepiped model.

For horizontal well pressure transient response, Goode and Thambynayagam[7] solved a model in Laplace space and inverted the solution using a numerical inverter. Their solution is very useful for pressure transient test diagnosis by identifying limiting flow regimes. Once these regimes become evident in a pressure transient test, the controlling variables may be calculated. For example, early-time radial flow may lead to the calculation of the product of the vertical permeability to the permeability normal to the well trajectory; late-time radial flow can allow the estimation of the product of the two horizontal permeabilities.

Previous work in pressure transient response of horizontal wells was presented by Daviau *et al.*[8] and Clonts and Ramey.[9] Kuchuk *et al.*[10] extended the Goode and Thambynayagam[7] approach to include constant pressure (top and/or bottom) boundaries.

Odeh and Babu[11] criticized these models, arguing that the actual presence of lateral boundaries may distort or completely mask several of the patterns implied by the infinite-acting boundaries of the pressure transient solutions. While the Odeh and Babu[11] contention is correct, clearly the pressure transient models are invaluable for flow-regime identification. Permeability calculations are not affected by boundary effects once the characteristic pressure and pressure responses of radial or linear flow are diagnosed convincingly. If these regimes do not appear, no calculations are possible with any model.

While other boundary effects have led to several and, at times, somewhat controversial results, the inner boundary condition (i.e., flow into the well) is even more interesting. The simplest model of flow into a well used in the past is that of uniform flux; i.e., the flow rate per unit well length is constant for each section of the well. A more realistic inner boundary condition would be one of uniform pressure (i.e., infinite conductivity of the wellbore).

Uniform flux solutions predict a well-flowing pressure drop that, in general, varies along the well. It is highest towards the center, decreasing considerably towards the well ends (see **Fig. 1**). To obtain a well bottomhole pressure, the Kuchuk *et al.*[10] approach averages the pressure along the well length. Babu and Odeh[4] take the pressure at the well midpoint; their model predicts a slightly larger pressure drop and, consequently, a slightly smaller productivity index than the one by Kuchuk *et al.*[10] The difference between these two approaches vanishes for fully penetrating wells but becomes increasingly obvious for smaller penetration.

For largely uniform pressure at the inner boundary (i.e., infinite conductivity well), the flux into the well varies. This has been observed in real wells (see **Fig. 2**).

None of the previous models can represent adequately well configurations that are becoming increasingly common today, such as multiple horizontal wells of arbitrary direction emanating from the same vertical well or open and close segments within the same horizontal well. Resolving these issues and presenting generalized forms of the productivity index relationships are the subjects of our paper.

Determination of the Well-Productivity Index

We use a well-productivity index, *J*, of the general form (in oilfield units)

$$J = \frac{q}{\bar{p} - p_{wf}} = \frac{\bar{k} x_e}{887.22 B \mu \left(p_D + \frac{x_e}{2\pi L} \sum s \right)}, \quad \ldots\ldots\ldots\ldots (1)$$

where $\bar{p}$ is the reservoir pressure and p_D is the dimensionless pressure whose calculation we expand upon in the Appendix. The summation Σs refers to the damage skin, turbulence, and/or other pseudoskin factors. For the remaining text, we will presume that $\Sigma s = 0$, although in any calculation we can readily account for it.

The generalized solution to the dimensionless pressure p_D encompasses early-time transients and all geometric and permeability interactions, culminating into pseudosteady state when all drainage boundaries are felt.

At that moment, the dimensionless pressure can be decomposed from one 3D to two 2D contributions. Because we are dealing large-

*Now with Veitsch-Radex AG, Vienna

Copyright 1996 Society of Petroleum Engineers

Original SPE manuscript received for review 16 September 1994. Paper peer approved 6 November 1996. Paper (SPE 27980) first presented at the 1994 University of Tulsa Centennial Petroleum Engineering Symposium held in Tulsa, 29–31 August.

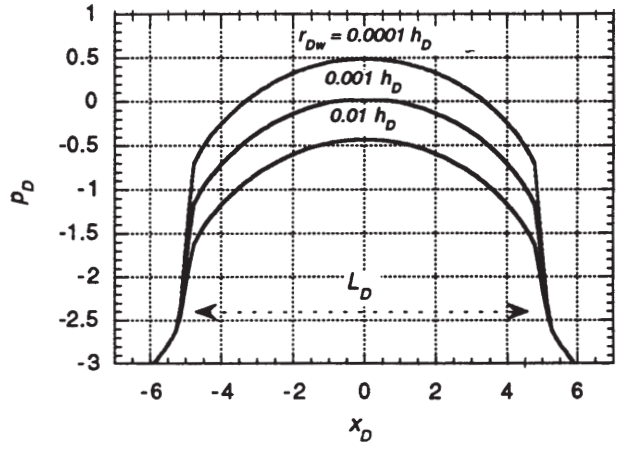

Fig. 1—Pseudosteady-state pressure profile along the well trajectory for uniform flux. Well length, $L_D = 10\ h_D$ (the well extends from $x_D = -5$ to $x_D = 5$, and the lateral boundaries are far away). Pressure is shown for three values of $r_{Dw} = 0.01\ h_D$, $0.001 h_D$ and $0.0001 h_D$. Note that even for very small h_D values the pressure varies considerably.

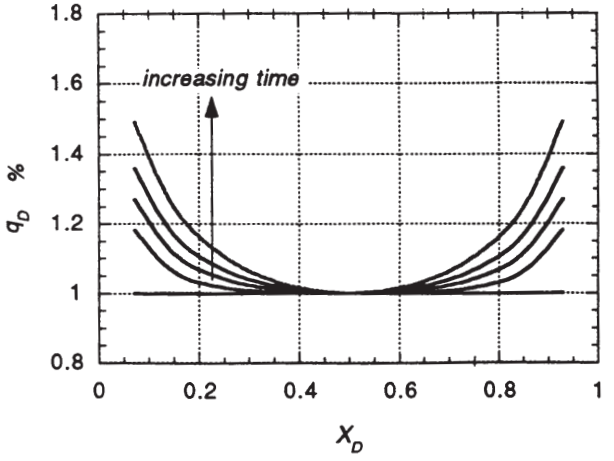

Fig. 2—Flux into a well (rate/length) with uniform pressure at different times. For small t_d flux is uniform. At the end of the early linear flow period the curve begins to develop sharp peaks at both ends.

ly with horizontal wells in this paper, it is convenient to characterize the horizontal plane by shape factors, while the vertical effects can be represented in the form of a skin effect.

Thus,

$$p_D = \frac{x_e C_H}{4\pi h} + \frac{x_e}{2\pi L} s_x , \quad \ldots\ldots\ldots\ldots\ldots\ldots\ldots\ldots\ldots\ldots (2)$$

where the skin effect, s_x, is (after Kuchuk *et al.*[10])

$$s_x = \ln\left(\frac{h}{2\pi r_w}\right) - \frac{h}{6L} + s_e , \quad \ldots\ldots\ldots\ldots\ldots\ldots\ldots\ldots\ldots\ldots (3)$$

and s_e, describing eccentricity effects in the vertical direction, is

$$s_e = \frac{h}{L}\left[\frac{2z_w}{h} - \frac{1}{2}\left(\frac{2z_w}{h}\right)^2 - \frac{1}{2}\right] - \ln\left[\sin\left(\frac{\pi z_w}{h}\right)\right]. \quad \ldots\ldots\ldots\ldots (4)$$

The value of s_e is negligible if the well is placed largely in the vertical middle of the reservoir.

To account for permeability anisotropy with k_x, k_y, and k_z in the x, y, and z direction, respectively, the following transformations must be introduced.[12]

Transformation for the Well.

Length:

$$L' = L\alpha^{-1/3}\beta. \quad \ldots\ldots\ldots\ldots\ldots\ldots\ldots\ldots\ldots\ldots\ldots\ldots\ldots\ldots (5)$$

Wellbore radius:

$$r_w' = r_w \frac{\alpha^{2/3}}{2}\left(\frac{1}{\alpha\beta} + 1\right), \quad \ldots\ldots\ldots\ldots\ldots\ldots\ldots\ldots\ldots\ldots (6)$$

$$\text{with } \alpha = \sqrt{\frac{(k_x k_y)^{1/2}}{k_z}} \quad \ldots\ldots\ldots\ldots\ldots\ldots\ldots\ldots\ldots\ldots (7)$$

$$\text{and } \beta = \left(\sqrt{\frac{k_y}{k_x}}\cos^2\varphi + \sqrt{\frac{k_x}{k_y}}\sin^2\varphi\right)^{1/2}. \quad \ldots\ldots\ldots\ldots (8)$$

Transformation for the Reservoir Dimensions.

$$x' = x\frac{\sqrt{k_y k_z}}{\bar{k}}, \quad \ldots\ldots\ldots\ldots\ldots\ldots\ldots\ldots\ldots\ldots\ldots\ldots\ldots\ldots (9)$$

$$y' = y\frac{\sqrt{k_x k_z}}{\bar{k}}, \quad \ldots\ldots\ldots\ldots\ldots\ldots\ldots\ldots\ldots\ldots\ldots\ldots\ldots\ldots (10)$$

$$z' = z\frac{\sqrt{k_x k_y}}{\bar{k}}, \quad \ldots\ldots\ldots\ldots\ldots\ldots\ldots\ldots\ldots\ldots\ldots\ldots\ldots\ldots (11)$$

$$\text{and } \bar{k} = \sqrt[3]{k_x k_y k_z}. \quad \ldots\ldots\ldots\ldots\ldots\ldots\ldots\ldots\ldots\ldots\ldots\ldots\ldots (12)$$

With these transformations and adjusting the well and reservoir variables, the p_D calculation can then proceed in the normal fashion.

Eqs. 1 to 4 are sufficient for the prediction of any single- or multiple-well configuration, and the general solutions described in the Appendix can handle all situations for infinite-acting, mixed, and no-flow boundaries. To demonstrate the utility of the approach, a few studies are presented here, including a table of shape factors for rapid approximations.

1. Pressure Transient Response—Flow Regime Identification. As mentioned earlier, the solutions by Goode and Thambynayagam[7] and Kuchuk *et al.*[10] have identified certain limiting flow regimes that, once diagnosed by a well test, can lead to the estimation of controlling variables, such as the appropriate permeability components. Odeh and Babu[11] stated that not all flow regimes are present in all cases and they are, of course, correct.

If the well is relatively short compared to the x_e dimension ($L < 0.2x_e$) and the reservoir thickness is not too small (e.g., $h > 0.05x_e$), then early-time radial, middle-time linear, and late-time pseudoradial flow are all likely to appear before pseudosteady state emerges. These trends are shown in **Fig. 3.**

If, however, the well length is large compared to the reservoir dimension, e.g., $L < 0.8x_e$, no late-time pseudoradial flow will appear, and the well will enter the pseudosteady-state condition after the linear flow period (**Fig. 4**).

Similarly, if the reservoir thickness is relatively small, no distinct early-time radial flow will appear, with the well entering linear flow directly. As can be surmised logically, the appearance of these flow regimes depends greatly on the relationships among the dominant dimensions, h, x_e, y_e, and L. The solutions presented in this paper can readily reproduce the appropriate trends for any geometric combinations.

2. Horizontal Plane Shape Factors. While any well and reservoir configuration solution can be handled rigorously, for quick calculations, it is convenient to use approximating shape factors. **Table 1** contains shape factors for relatively common configurations. These shape factors can be used in Eq. 2, along with a calculation of the vertical configuration skin effect (Eqs. 3 and 4) for the determina-

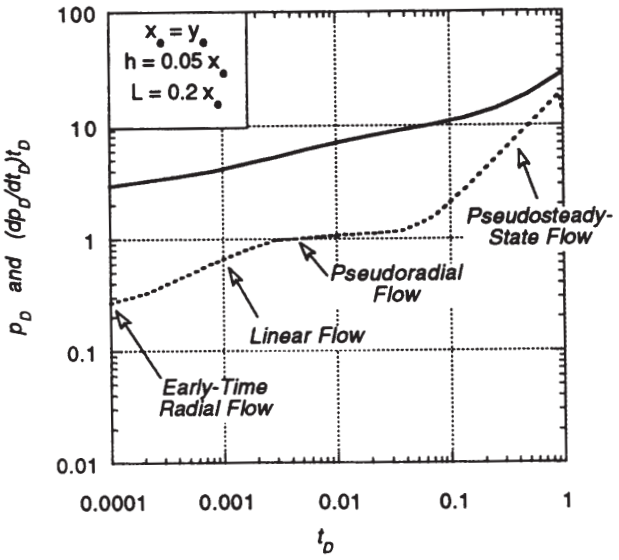

Fig. 3—Flow regimes of a mildly laterally penetrating horizontal well.

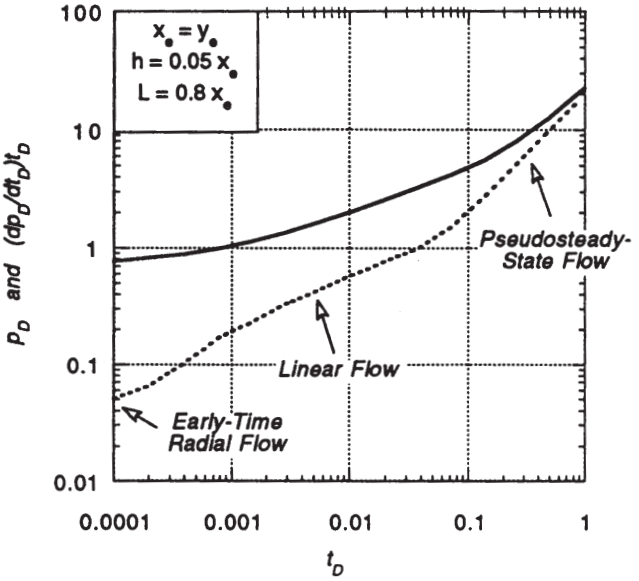

Fig. 4—Flow regimes of an almost fully penetrating horizontal well.

tion of the p_D. Then, the productivity index can be determined readily from Eq. 1.

An example calculation is presented below.

Suppose that a horizontal well 1,500 ft long is in a 1×2 reservoir with $x_e = 2{,}000$ ft and $y_e = 4{,}000$ ft. If $h = 20$ ft, $r_w = 0.4$ ft, k (isotropic throughout) = 10 md, $B_o = 1.25$ resbbl/STB, and $\mu_o = 1$ cp, calculate the well-productivity index. Assume that the well is in the vertical middle of the reservoir ($s_e = 0$).

From Eq.3,

$$s_x = \ln\left[\frac{20}{2\pi(0.4)}\right] - \frac{20}{(6)1500} = 2.07, \quad \ldots\ldots\ldots\ldots\ldots (13)$$

using Table 1 with $2x_e = y_e$ and $L/x_e = 0.75$ $C_H = 2.53$.

Thus, from Eq. 2,

$$p_D = \frac{(2000)(2.53)}{4\pi(20)} + \frac{(2000)(2.07)}{2\pi(1500)} = 20.58, \quad \ldots\ldots\ldots (14)$$

and, finally, from Eq. 1

$$J = \frac{(10)(2000)}{(887.22)(1.25)(1)(20.58)} = 0.88 \text{ STB/D/psi}. \quad \ldots\ldots (15)$$

3. Effect of Orientation on Horizontal Well. Frequently, formations are permeability-anisotropic in the horizontal plane.[13] Drilling a horizontal well in the appropriate direction can be critical. The determination of the maximum and minimum horizontal permeability directions, usually coinciding with the maximum and minimum horizontal stress directions, must be done before a horizontal well is drilled. In a new reservoir, this can be accomplished in a vertical pilot hole with a variety of formation evaluation technologies.

Here, a study is presented showing horizontal well-productivity index vs. time as a function of well orientations. Pertinent variables include $k_x = 10$ md, $k_y = 2$ md, $k_z = 1$ md, $x_e = y_e = 2{,}000$ ft, $h = 50$ ft, and $L = 1200$ ft. The well is rotated at the center of the drainage area and is at the vertical middle of the reservoir. **Fig. 5** presents the results, demonstrating the importance of proper well orientation. For this case study, the ratio of the productivity indexes between the best (normal to k_x) and the worst (normal to k_y) is 1.6 at 2 months. Permeability anisotropies in the horizontal plane of 3:1 or larger are considered common and, therefore, proper horizontal well orientation can mean very large differences in early-time well performance.[14] Of course, after pseudosteady-state conditions appear, these productivity index differences vanish. However, transient productivity indexes can mean the difference between an economically attractive well and one that is not. This would be particularly true for large drainage areas.

The calculation presented here can be done in longhand using the transformations in Eqs. 5 to 12 and then following the procedure outlined in Section #2.

TABLE 1—HORIZONTAL PLANE SHAPE FACTORS

		L/x_e	C_H
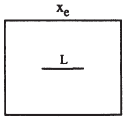	$x_e = 4y_e$	0.25	3.77
		0.5	2.09
		0.75	1.00
		1	0.26
	$x_e = 2y_e$	0.25	3.19
		0.5	1.80
		0.75	1.02
		1	0.52
	$x_e = y_e$	0.25	3.55
		0.5	2.21
		0.75	1.49
		1	1.04
	$2x_e = y_e$	0.25	4.59
		0.5	3.26
		0.75	2.53
		1	2.09
	$4x_e = y_e$	0.25	6.69
		0.5	5.35
		0.75	4.63
		1	4.18
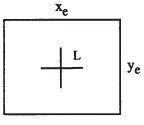	$x_e = y_e$	0.25	2.77
		0.5	1.47
		0.75	0.81
		1	0.46
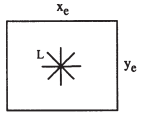	$x_e = y_e$	0.25	2.66
		0.5	1.36
		0.75	0.69
		1	0.32
		φ	
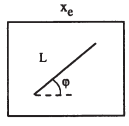	$x_e = y_e$	0	1.49
	$L/x_e = 0.75$	30	1.48
		45	1.48
		75	1.49
		90	1.49

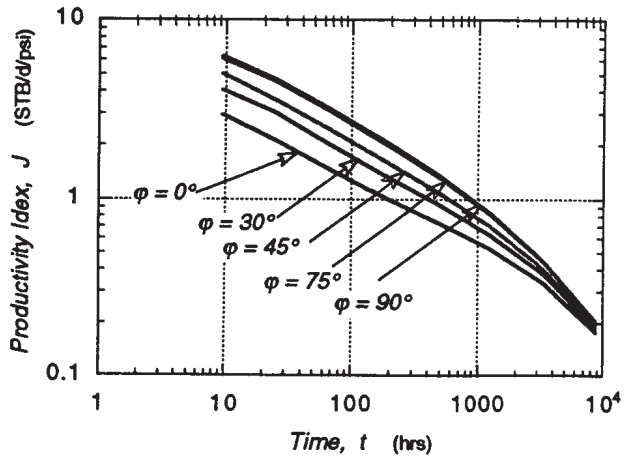

Fig. 5—Productivity index vs rotation of a horizontal well in a permeability-anisotropic reservoir.

Discussion

We summarize our concept here. The dimensionless pressure of a point source in a box with no-flow boundaries can be written in an integral form, Eq. A-10 in the Appendix. For early times, contributions to the integral are evaluated more efficiently by Eq. A-8. Certainly, the careful switching between different solutions imposes some administrative complications for a computer program. On the other hand, we want to emphasize that a solution calculated by this strategy will be exact up to any prescribed accuracy (i.e., so far there are no simplifying assumptions involved).

Several approaches yield accurate approximations. For the specific assumptions of a well parallel to the y-axis and uniform flux (Eq. A-6), Babu and Odeh[4] worked out a solution for the pseudosteady-state pressure at any point in the reservoir.

Their solution starts with a triple sum of Green's functions, doubly integrated over y and t. Suitable simplifications reduce this expression to a couple of terms that involve (still lengthy) summation formulas. By similar methods, Odeh and Babu[11] give transient pressures as well. Kuchuk *et al.*[10] find the solution for transient and pseudosteady-state pressure using Laplace transformations.

The above works are outstanding contributions, presenting closed-form analytical expressions and must be considered as seminal work. We believe, though, that analytical approaches have reached their limitations. These can be overcome and solutions can be generalized with the methodology presented in our paper. Our work has other parallel works in the literature, notable among which is the solution by Cinco-Ley and Meng[15] for hydraulically fractured wells in double porosity media.

Conclusions

A methodology of calculating well performance of arbitrarily oriented, single- or multiple-well configurations, based on carefully evaluated analytical solutions, has been introduced. The approach is general, readily reproduces well-known analytical solutions, and can be used for transient, mixed-, and no-flow boundary conditions. Several applications including simple, horizontal plane shape factors have been presented in this paper.

Nomenclature

B = formation volume factor, bbl/STB
C_H = shape factor
c_t = total compressibility, psi^{-1}
h = reservoir thickness, ft
J = productivity index, STB/D/psi
k = permeability, md
$\bar{k}$ = average permeability, md
L = well length, ft
$\bar{p}$ = average reservoir pressure, psi
p_{wf} = bottomhole flowing pressure, psi
q = flowrate, STB/D
r_w = wellbore radius, ft
s = skin effect
t = time, hrs
x_e = extent of drainage area in x-direction, ft
y_e = extent of drainage area in y-direction, ft
z_w = distance of well from middle of reservoir, ft
α,β = coordinate transformation factors
ϕ = porosity
μ = viscosity, cp
φ = azimuth of well trajectory (relative to x-axis)

Subscripts

D = dimensionless
w = well

Acknowledgments

The authors would like to thank W. Winkler for his invaluable help with this paper.

References

1. Borisov, J.P.: *Oil Production Using Horizontal and Multiple Deviation Wells,* Nedra, Moscow (1964). Translated by J. Strauss, S.D. Josh (ed.), Phillips Petroleum Co., the R&D Library Translation, Bartlesville, Oklahoma (1984).
2. Joshi, S.D.: "Augmentation of Well Productivity With Slant and Horizontal Wells," *JPT* (June 1988) 729–739.
3. Economides, M.J., Deimbacher, F.X., Brand, C.W., and Heinemann, Z.E.: "Comprehensive Simulation of Horizontal-Well Performance," *SPEFE* (December 1991) 418–426.
4. Babu, D.K. and Odeh, A.S.: "Productivity of a Horizontal Well," *SPERE* (November 1989) 417–421.
5. Dietz, D.N.: "Determination of Average Reservoir Pressure From Build-Up Surveys," *SPEJ* (June 1965) 117–122; *Trans.,* AIME, **261.**
6. Matthews, C.S., Brons, F., and Hazebroek, P.: "A Method for Determination of Average Pressure in a Bounded Reservoir," *Trans.,* AIME (1955) **204.**
7. Goode, P.A. and Thambynayagam, R.K.M.: "Pressure Drawdown and Buildup Analysis of Horizontal Wells in Anisotropic Media," *SPEFE* December 1987) 683–697; *Trans.,* AIME, **283.**
8. Daviau, F., Mouronval, G., Bourdarot, G., and Curutchet, P.: "Pressure Analysis for Horizontal Wells," paper SPE 14251, 1985.
9. Clonts, M.D. and Ramey, H.J. Jr.: "Pressure Transient Analysis for Wells With Horizontal Drainholes," paper SPE 15116, 1986.
10. Kuchuk, F.J., Goode, P.A., Brice, B.W., Sherrard, D.W., and Thambynayagam, R.K.M. "Pressure Transient Analysis and Inflow Performance for Horizontal Wells," paper SPE 18300, 1988.
11. Odeh, A.S. and Babu, D.K.: "Transient Flow Behavior of Horizontal Wells: Pressure Drawdown and Buildup Analysis," *SPEFE* (March 1990) 7–15.
12. Besson, J.: "Performance of Slanted and Horizontal Wells on an Anisotropic Medium," paper SPE 20965, 1990.
13. Buchsteiner, H., Warpinski, N.R., and Economides, M.J.: "Stress Induced Permeability Reduction in Fissured Reservoirs," paper SPE 26513, 1993.
14. Brown, J.E. and Economides, M.J.: "An Analysis of Hydraulically Fractured Horizontal Wells," paper SPE 24322, 1992.
15. Cinco-Ley, H. and Meng, H.Z.: "Pressure Transient Analysis of Wells With a Finite Conductivity Fracture in Double Porosity Reservoirs," paper SPE 18172, 1988.
16. Goode, P.A. and Wilkinson, D.J.: "Inflow Performance of Partially Open Horizontal Wells," *JPT* (August 1991) 983–987.
17. Carslaw, H.S. and Jaeger, J.C.: *Conduction of Heat In Solids*, Oxford University Press, Oxford, 1959.
18. Press, W.H., Flannery, B.P.. Teukolsky, S.A., and Vetterling, W.T.: *Numerical Recipes*, Cambridge University Press, Cambridge, 1986.

Appendix A—Analytical and Numerical Solutions

Mathematical Representation. The basic equation that governs single-phase flow of a slightly compressible fluid in a porous medium is (in dimensionless variables)

$$\frac{\partial^2 p_D}{\partial x_D^2} + \frac{\partial^2 p_D}{\partial y_D^2} + \frac{\partial^2 p_D}{\partial z_D^2} = \frac{\partial p_D}{\partial t_D}. \quad \ldots\ldots\ldots\ldots\ldots\ldots \text{(A-1)}$$

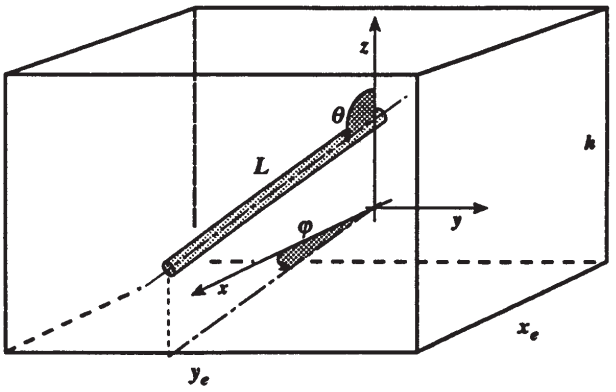

Fig. A-1—Basic parallelepiped model with appropriate coordinates (after Besson[12]).

We seek solutions for the dimensionless pressure p_D depending on dimensionless space and time coordinates, $p_D = p_D(x_D, y_D, z_D, t_D)$.

Eq. 1 relates p_D to the real flowing bottomhole pressure p_{wf}. To convert the space coordinates or lengths to their dimensionless equivalent, they are scaled by x_e (the reservoir length in the x-direction—see **Fig. A-1**),

$$x_D = x/x_e,\ y_D = y/x_e,\ z_D = z/x_e. \quad \ldots\ldots\ldots\ldots\ldots \text{(A-2)}$$

Time is scaled by

$$t_D = 0.000264\,\frac{t}{x_e^2}\,\frac{k}{\mu c_t \phi}, \quad \ldots\ldots\ldots\ldots\ldots\ldots\ldots \text{(A-3)}$$

where 0.000264 is the conversion factor for t measured in hours, and field units for k, x_e, μ, and c_t. There is nothing special about the choice of x_e for scaling lengths. Indeed, any other length will do instead, as long as it is used consistently in Eqs. A-2 and A-3. A subscript D will throughout this Appendix denote the dimensionless equivalent for any variable.

Exterior boundary conditions for our model (Fig. A-1) are no-flow across the walls of the box with sides of dimensionless length x_{De}, y_{De}, z_{De}, thus

$$\frac{\partial p_D}{\partial x_D} = 0 \text{ at } x_D = 0 \text{ and } x_D = 1, \quad \ldots\ldots\ldots\ldots \text{(A-4a)}$$

$$\frac{\partial p_D}{\partial y_D} = 0 \text{ at } y_D = 0 \text{ and } y_D = y_{De}, \quad \ldots\ldots\ldots\ldots \text{(A-4b)}$$

$$\frac{\partial p_D}{\partial z_D} = 0 \text{ at } z_D = 0 \text{ and } z_D = z_{De}. \quad \ldots\ldots\ldots\ldots \text{(A-4c)}$$

The initial condition is

$$p_D = 0 \text{ for } t = 0 \quad \ldots\ldots\ldots\ldots\ldots\ldots\ldots\ldots \text{(A-5)}$$

everywhere inside the box.

Boundary Conditions at the Wellbore. Assume that in the box there is a line source following some trajectory. This trajectory may be a straight line segment parallel to the x- or y-axes,[4,10] or the straight line segment may be slanted and rotated with respect to the coordinate axes. More generally, the trajectory may not be straight at all. For example, a sequence of point coordinates may define the well's trajectory. The well, then, is a cylindrical or tubular region of radius r_{Dw} around the trajectory. We apply two types of boundary conditions at the surface of this region (i.e., at the well surface).

The boundary condition for uniform flux imposes a constant pressure derivative normal to the well surface. Assuming a flow rate q_D and well length L_D,

$$\frac{\partial p_D}{\partial r_D} = const = \frac{2\pi q_D}{L_D} \text{at } r_D = r_{Dw}, \quad \ldots\ldots\ldots\ldots \text{(A-6a)}$$

$$\text{for } r_D = \sqrt{x_D^2 + y_D^2 + z_D^2}. \quad \ldots\ldots\ldots\ldots\ldots\ldots \text{(A-6b)}$$

The second type imposes uniform well flowing pressure, p_{Dwf},

$$p_D = const = p_{Dwf} \text{ at } r_D = r_{Dw}. \quad \ldots\ldots\ldots\ldots\ldots \text{(A-7)}$$

Neither condition is entirely realistic. For uniform flux, the pressure at the wellbore is not constant (see Fig. 1); the pressure drop along the well may be a significant part of the total pressure drop in the reservoir. The problem, then, is to define a value for p_{Dwf}. One possibility is to use the pressure at the midpoint of the well length.[4] Another possibility to define p_{Dwf} as the average pressure along the well.[10]

For uniform pressure, the flux into the well varies. Both ends of the well produce proportionally more than the middle section (Fig. 2). This is indeed the case for real wells. It is the reason why partial completions at the ends of the wellbore are more efficient than the same length of completion, distributed equally along the well.[16] Still, this boundary condition does not account for pressure loss in the wellbore; it assumes infinite conductivity in the well. Closed-form analytical solutions for the general problem of Eq. A-1, with initial and boundary conditions of Eqs. A-4, A-5, A-6, or A-7 are not known (and, given the complexity of solutions even in much simpler cases, are unlikely to exist).

Our Approach. We pursue a different approach. It involves three steps.

1. Obtain a solution for $p_D(x_D, y_D, z_D, t_D)$ for a point source with unit strength, located somewhere inside the box at x_{D0}, y_{D0}, z_{D0}. Represent the solution in a form that a computer can evaluate fast. Our model relies strongly on the ability to compute this point-source solution accurately and fast. Let us denote this solution in the style of a FORTRAN function as $\text{cpsrc}(x_D, y_D, z_D, x_{D0}, y_{D0}, z_{D0}, t_D)$, where cpsrc stands for continuous point source.

2. For a line source with uniform flux and unit strength, integrate the solution for the point source numerically along the well trajectory. (Some care is necessary to make numerical integration work well; we will discuss the fine points of our implementation later.) In this way, we form the solution of a straight line source of unit strength, located between the points (x_{D0}, y_{D0}, z_{D0}) and (x_{D1}, y_{D1}, z_{D1}) and evaluated at a point (x_D, y_D, z_D) inside the reservoir and at time t_D. In FORTRAN-like style, let us call it $\text{clsrc}(x_D, y_D, z_D, x_{D0}, y_{D0}, z_{D0}, x_{D1}, y_{D1}, z_{D1}, t_D)$. clsrc stands for continuous line source.

3. For a line source with constant pressure, split the well into n segments. Treat each segment as a line source with uniform flux, using the solution above. Assign a rate to each segment so that the individual rates sum up to one. Superpose the solutions and adjust the individual rates so that the pressures at the midpoint of each segment are all the same. "Adjusting" means there are $n+1$ parameters in the system, the rates for each of the n segments and the common well flowing pressure. They are, correspondingly, n linear equations that link the pressure at each segment to the individual rates of the segments and one equation stating that the rates sum up to 1. We will describe the process in some more detail below.

Solutions for a Point Source. We describe the evaluation of the function $\text{cpsrc}(x_D, y_D, z_D, x_{D0}, y_{D0}, z_{D0}, t_D)$, i.e., the transient dimensionless pressure at position (x_D, y_D, z_D), resulting from a point source of unit strength located at (x_{D0}, y_{D0}, z_{D0}) in a rectangular box with no-flow boundaries. We will build this function using several different solutions.

One basic building block is the solution for an instantaneous point source of unit strength in the 1D region $0 \le x_D \le 1$, no-flow boundaries at $x_D = 0$ and $x_D = 1$. Carslaw and Jaeger[17] give two representations of this solution. By the method of images,

$$p_D = \frac{1}{\sqrt{4\pi t_D}} \sum_{n=-\infty}^{\infty} e^{-\left(2n + x_{D0} - x_D\right)^2/4t} + e^{-\left(2n - x_{D0} - x_D\right)^2/4t}. \quad \ldots\ldots\ldots\ldots\ldots \text{(A-8)}$$

The second form uses Fourier series,

$$p_D = 1 + 2\sum_{n=1}^{\infty} e^{-n^2\pi^2 t_D} \cos(n\pi x_D)\cos(n\pi x_{D0}). \quad \ldots\ldots \text{(A-9)}$$

Both forms represent the same, unique solution. The first one, however, converges rapidly for small t_D but involves lengthy summations for large t_D. Fortunately, the second form complements this behavior; i.e., it converges slowly for small t_D and rapidly later on. There is an optimum time of the order $t_D = \frac{1}{4}\pi$, when to switch from one equation to the other.

A computer routine ips1 (x_D, x_{D0}, t_D) that uses the proper equation will, for a relative accuracy of 10^{-6}, never have to sum more than eight exponential terms (and much less for most values of t_D).

The 3D solution $\text{cpsrc}(x_D, y_D, z_D, x_{D0}, y_{D0}, z_{D0}, t_D)$ is the product of three 1D solutions, integrated over time.

$$p_D = \frac{1}{x_{De} y_{De} z_{De}} \int_0^{t_D} \text{ips1}\left(\frac{x_D}{x_{De}}, \frac{x_{D0}}{x_{De}}, \frac{t_D}{x_{De}^2}\right) \times$$

$$\text{ips1}\left(\frac{y_D}{y_{De}}, \frac{y_{D0}}{y_{De}}, \frac{t_D}{y_{De}^2}\right) \times$$

$$\text{ips1}\left(\frac{z_D}{z_{De}}, \frac{z_{D0}}{z_{De}}, \frac{t_D}{z_{De}^2}\right) dt_D \,. \quad \text{..... (A-10)}$$

If the computer can evaluate ipsi ( ) fast and accurately, then any subroutine for adaptive quadrature can perform the time integration. Our implementation uses an adaptive Romberg quadrature (see, e.g., Press *et al.*[18]) on subintervals that get larger as t_D increases.

Still, however, this evaluation is computationally long. Savings are possible for small and large t_D.

First, it does not make sense to carry out explicitly the integration in Eq. A-10 for $t_D \gg \max(x_{De}^2, y_{De}^2, z_{De}^2)$. For large t_D, in the pseudo-steady-state regime, ips1() evaluates to 1, and the contribution to the integral in Eq. A-10 from time t_{D1} to t_{D2} is simply

$$\frac{t_{D2} - t_{D1}}{x_{De} y_{De} z_{De}} \text{ for } t_{D1}, t_{D2} \gg 1. \quad \text{..... (A-11)}$$

For small t_D, up to the late radial flow period, p_D does not feel lateral boundaries. In this case, the solution that can be used is the one for a continuous point source, unit strength, between parallel planes with no-flow boundaries at $z_D = 0$ and $z_D = z_{De}$.

Again, Carslaw and Jaeger[16] list two solutions. For small t_D, summing over images converges rapidly,

$$p_D = \frac{1}{\sqrt{4\pi r_D}} \sum_{n=-\infty}^{\infty} \text{erfc}\left[\sqrt{\frac{\rho_D^2 + (2nz_{De} + z_{D0} - z_D)^2}{4t_D}}\right] +$$

$$+ \text{erfc}\left[\sqrt{\frac{\rho_D^2 + (2nz_{De} - z_{D0} - z_D)^2}{4t_D}}\right]. \quad \text{..... (A-12)}$$

Here $\rho_D^2 = (x_D - x_{D0})^2 + (y_D - y_{D0})^2$, the radial distance in the x-y-plane.

The Fourier series solution is

$$p_D = \frac{1}{4\pi z_e} \int_0^{t_D} e^{-\rho_D^2/4t}$$

$$\left(1 + 2\sum_{n=1}^{\infty} e^{-\frac{n^2\pi^2}{z_e^2} t_D} \cos\frac{n\pi z_D}{z_{De}} \cos\frac{n\pi z_{D0}}{z_{De}}\right) dt_D \,. \quad \text{..... (A-13)}$$

When

$$t_{D\varepsilon} > \left(\frac{z_{De}}{\pi}\right)^2 \ln\frac{2}{\varepsilon}, \quad \text{..... (A-14)}$$

the contribution from the exponential term in the infinite sum is smaller than an accuracy threshold ε. The contribution to the integral in Eq. A-13 from $t_{D\varepsilon}$ to t_D is then evaluated by the familiar Exponential Integral,

$$-Ei\left(\frac{-\rho_D^2}{4t_D}\right) + Ei\left(\frac{-\rho_D^2}{4t_{D\varepsilon}}\right). \quad \text{..... (A-15)}$$

For the contribution from 0 to t_D, evaluate Eq. A-12 at $t_{D\varepsilon}$ and add to Eq. A-15.

Line Source With Uniform Flux. The solution for a continuous line source with unit strength is defined as the integral over the point source solution. Numerical integration of cpsrc would give p_D. For a point at the well surface (i.e. at a small distance r_{wD} from the line source), however, the integrand will have a sharp peak. Straightforward numerical integration of cprsc then either gives poor results or takes many computational steps. The trick here is to subtract a term $\frac{1}{4}\pi r_D$ from the point source solution, thus removing the almost singular behavior of the integrand. The remainder varies smoothly and presents no problem to an adaptive quadrature scheme. The $\frac{1}{4}\pi r_D$-contribution can be integrated analytically. This is the steady-state solution for a line source. The subroutine that implements ideas to give p_D at position x_D, y_D, z_D for a line source between the points x_{D0}, y_{D0}, z_{D0} and x_{D1}, y_{D1}, z_{D1} at time t_D is called $\text{clsrc}(x_D, y_D, z_D, x_{D0}, y_{D0}, z_{D0}, x_{D1}, y_{D1}, z_{D1}, t_D)$.

Line Source With Uniform Pressure. Our approach to split the well in n segments and to adjust rates so that the pressures in all segments become equal, is similar to the methods of Besson.[12] For a prescribed total flow rate, the solution of n+1 linear equations gives the distribution of the rate among the segments in the well and the well flowing pressure. The rate distribution varies with time. It is uniform for very small t_D but spikes at the ends of the well develop quickly, after the early linear flow period. Thus, an additional time-stepping scheme in our program captures this phenomenon.

SI Metric Conversion Factors

cp × 1.0*	E−03 = Pa·s
ft × 3.048*	E−01 = m
psi × 6.894 757	E+00 = kPa

*Conversion factor is exact. **SPEFE**

Michael J. Economides is the Noble Professor of Petroleum Engineering at Texas A&M U. in College Station. Previously, he was professor of petroleum engineering and Director of the Inst. of Drilling & Production at Mining U. Leoben in Austria. Economides holds both BS and MS degrees in chemical engineering from the U. of Kansas and a PhD degree in petroleum engineering from Stanford U. He was a 1994 Distinguished Member, 1992–93 Review Chairman, and 1991–92 Distinguished Lecturer. He was also a Technical Editor during 1982–84, 1984–86, and 1991–92. **Clemens Brand** is associate professor at the Inst. of Applied Mathematics at Mining U. of Leoben in Austria. His research responsibilities include numerical grid generation, discretization methods, and linear solvers. He holds MS and PhD degrees from the U. of Vienna. **Thomas P. Frick** works with Veitsch-Radex AG in Vienna. Previously, he was an assistant professor at Mining U. Leoben, where he earned a PhD degree in petroleum engineering.

Economides Brand Frick